

## Article

# The Magnetostriction of Amorphous Magnetic Microwires: The Role of the Local Atomic Environment and Internal Stresses Relaxation

Valentina Zhukova <sup>1,2,3</sup> , Alfonso García-Gómez <sup>1,2,3</sup> , Alvaro Gonzalez <sup>1,2,3</sup> , Margarita Churyukanova <sup>4</sup>, Sergey Kaloshkin <sup>4</sup>, Paula Corte-Leon <sup>1,2,3</sup> , Mihail Ipatov <sup>1,2,3</sup> , Jesus Olivera <sup>5</sup> and Arcady Zhukov <sup>1,2,3,6,\*</sup> 

- <sup>1</sup> Department Advanced Polymers and Materials: Physics, Chemistry and Technology, Faculty of Chemistry, University of the Basque Country, UPV/EHU, 20018 San Sebastian, Spain; valentina.zhukova@ehu.es (V.Z.); alfonso.garciag@ehu.es (A.G.-G.); alvaro.gonzalezv@ehu.es (A.G.); paula.corte@ehu.es (P.C.-L.); mihail.ipatov@ehu.es (M.I.)
- <sup>2</sup> Department Applied Physics I, EIG, University of the Basque Country, UPV/EHU, 20018 San Sebastian, Spain
- <sup>3</sup> EHU Quantum Center, University of the Basque Country, UPV/EHU, 20018 San Sebastian, Spain
- <sup>4</sup> Department of Physical Chemistry, National University of Science and Technology «MISIS», Leninsky Avenue, 4, 119049 Moscow, Russia; mch@misis.ru (M.C.); kaloshkin@misis.ru (S.K.)
- <sup>5</sup> Facultad de Ciencias, Instituto de Física, Universidad Autónoma de Santo Domingo, Santo Domingo 10105, Dominican Republic; jesus.oliveradga@gmail.com
- <sup>6</sup> IKERBASQUE, Basque Foundation for Science, 48011 Bilbao, Spain
- \* Correspondence: arkadi.joukov@ehu.es; Tel.: +34-943-01-8611

**Abstract:** We studied the magnetostriction coefficients,  $\lambda_s$ , Curie temperature,  $T_c$ , and their dependence on annealing conditions in  $\text{Fe}_{47}\text{Ni}_{27}\text{Si}_{11}\text{B}_{13}\text{C}_2$  and  $\text{Co}_{67}\text{Fe}_{3.9}\text{Ni}_{1.5}\text{B}_{11.5}\text{Si}_{14.5}\text{Mo}_{1.6}$  amorphous glass-coated microwires with rather different character of hysteresis loops. A positive  $\lambda_s \approx 20 \times 10^{-6}$  is observed in as-prepared  $\text{Fe}_{47}\text{Ni}_{27}\text{Si}_{11}\text{B}_{13}\text{C}_2$ , while low and negative  $\lambda_s \approx -0.3 \times 10^{-6}$  is obtained for  $\text{Co}_{67}\text{Fe}_{3.9}\text{Ni}_{1.5}\text{B}_{11.5}\text{Si}_{14.5}\text{Mo}_{1.6}$  microwire. Annealing affects the magnetostriction coefficients and Curie temperatures,  $T_c$ , of both  $\text{Fe}_{47}\text{Ni}_{27}\text{Si}_{11}\text{B}_{13}\text{C}_2$  and  $\text{Co}_{67}\text{Fe}_{3.9}\text{Ni}_{1.5}\text{B}_{11.5}\text{Si}_{14.5}\text{Mo}_{1.6}$  glass-coated microwires in a similar way. Observed dependencies of hysteresis loops,  $\lambda_s$  and  $T_c$  on annealing conditions are discussed in terms of superposition of internal stresses relaxation and structural relaxation of studied microwires. We observed linear  $\lambda_s$  dependence on applied stress,  $\sigma$ , in both studied microwires. A decrease in the magnetostriction coefficient upon applied stress is observed for Co-rich microwires with low and negative magnetostriction coefficient. On the contrary, for Fe-Ni-rich microwires with a positive magnetostriction coefficient, an increase in the magnetostriction coefficient with applied stress is observed. The observed results are discussed considering the internal stresses relaxation and short range atomic rearrangements induced by annealing on hysteresis loops, magnetostriction coefficients and Curie temperatures of studied microwires.

**Keywords:** amorphous magnetic materials; coercive force; magnetic hysteresis; magnetostriction



**Citation:** Zhukova, V.; García-Gómez, A.; Gonzalez, A.; Churyukanova, M.; Kaloshkin, S.; Corte-Leon, P.; Ipatov, M.; Olivera, J.; Zhukov, A. The Magnetostriction of Amorphous Magnetic Microwires: The Role of the Local Atomic Environment and Internal Stresses Relaxation. *Magnetochemistry* **2023**, *9*, 222. <https://doi.org/10.3390/magnetochemistry9100222>

Academic Editors: Krzysztof Chwastek and Carlos J. Gómez García

Received: 28 July 2023

Revised: 20 September 2023

Accepted: 16 October 2023

Published: 20 October 2023



**Copyright:** © 2023 by the authors. Licensee MDPI, Basel, Switzerland. This article is an open access article distributed under the terms and conditions of the Creative Commons Attribution (CC BY) license (<https://creativecommons.org/licenses/by/4.0/>).

## 1. Introduction

Magnetostriction,  $\lambda_s$ , refers to the behavior of a magnetic material that undergoes either expansion or contraction in the direction of magnetization when exposed to a magnetic field [1,2]. The  $\lambda_s$  can be either positive or negative, depending on whether the magnetostrictive effect leads to expansion or compression, respectively.

In amorphous alloys, magnetostriction is a phenomenon that relates to the deformation or change in shape of the material in response to an applied magnetic field. Unlike crystalline materials, amorphous alloys lack of long-range periodic atomic structure and instead have a disordered arrangement of atoms. In the absence of defects typical for crystalline materials (grain boundaries, dislocations, texture, etc.) the magnetoelastic anisotropy plays the determining role in magnetic softness of amorphous alloys [3–6]. The

magnetoelastic anisotropy,  $K_{me}$ , is determined by the magnetostriction coefficient,  $\lambda_s$ , as well as by the stress,  $\sigma$ , [3,4]. It is commonly accepted that in amorphous alloys the  $\lambda_s$  is influenced by the chemical composition: for Fe-rich compositions the  $\lambda_s$  is positive (up to  $40 \times 10^{-6}$ ) and large, while for Co-rich amorphous alloys  $\lambda_s$  is negative (up to  $-5 \times 10^{-6}$ ). Consequently, near-zero  $\lambda_s$  values have been achieved in  $\text{Co}_x\text{Fe}_{1-x}$  ( $0 \leq x \leq 1$ ) or  $\text{Co}_x\text{Mn}_{1-x}$  ( $0 \leq x \leq 1$ ) alloys  $0.03 \leq x \leq 0.08$  [3–5]. In such amorphous alloys with vanishing  $\lambda_s$  values, better magnetic softness is commonly reported [3–6].

However, magnetostriction of amorphous alloys is influenced by the local atomic environments, by the presence of clusters and even by stresses [7–9]. Thus, clusters are localized regions of atoms that exhibit different magnetic properties compared to the surrounding material. These clusters can arise due to variations in composition or local atomic arrangements within the amorphous structure. When an external mechanical stress is applied to an amorphous alloy with clusters, the magnetic moments within the clusters align with the stress direction, causing a local deformation or strain in the material. In the two-ion model, the strain experienced by one ion can affect the magnetic moment of the neighboring ion and vice versa. This coupling between strain and magnetism leads to changes in the magnetic properties of the material, including its magnetostriction [7].

Research on amorphous magnetic wires has attracted considerable attention owing to unusual magnetic properties, such as magnetic bistability related to fast magnetization switching through the fast domain wall (DW) propagation, superior magnetic softness or the giant magnetoimpedance (GMI) effect [4,10–12]. Such magnetic properties have been proposed for numerous applications in magnetic and/or magnetoelastic sensors and devices [4,8–10]. While the better magnetic softness and the highest GMI effect are commonly reported in magnetic wires with vanishing  $\lambda_s$ , spontaneous magnetic bistability is usually reported for magnetostrictive compositions of amorphous wires [4,10–12].

One of the recent tendencies in amorphous materials is the development of low dimensional amorphous materials with enhanced physical (mechanical, corrosion) properties and biocompatibility [4,6,11]. Therefore, studies of glass-coated microwires with unusual combination of physical properties, such as enhanced mechanical and corrosion properties, biocompatibility together with excellent magnetic softness with coercivities up to 2 A/m and high magnetoimpedance effect have attracted substantial attention [4,6,11].

The peculiarity of glass-coated microwires is the presence of the glass-coating intrinsically related to the fabrication method [4,6,11]. Such composite origin of glass-coated microwires is associated with high values of internal stresses in glass-coated microwires, discussed elsewhere [13–17]. Although there are several origins of the internal stresses in amorphous microwires, the main contribution is related with the difference in thermal expansion coefficients of metallic alloy and glass coating [13–17].

The magnetostriction coefficient plays a significant role in determining the domain structure and hysteresis loop characteristics of glass-coated microwires. In compositions with low magnetostriction, the stress dependence of magnetostriction, whether applied or internal, becomes relevant. This stress dependence has been described as [8,9]:

$$\lambda_s(\sigma) = \lambda_s(0) - B\sigma \quad (1)$$

Here,  $\lambda_s(\sigma)$  represents the magnetostriction coefficient under stress,  $\lambda_s(0)$  is the magnetostriction coefficient at zero stress,  $B$  is a positive coefficient of the order  $10^{-10}$  MPa, and  $\sigma$  represents the applied or internal stresses. The change in magnetostriction can be attributed to the presence of applied stresses ( $\sigma_{appl}$ ), internal stresses ( $\sigma_i$ ), or both ( $\sigma$ ).

Mechanical stresses play a significant role in modifying the magnetic properties of ferromagnetic materials. Alongside magnetic field and temperature, they are a crucial factor influencing magnetic properties. This phenomenon is commonly employed in stress and torsion sensors, where the variation in the material's magnetic properties is utilized for sensing purposes [5–8,18–22]. Magnetostriction also has an impact on various inductive or transport magnetic effects [20–22].

Recently, studies of glass-coated magnetic microwires have attracted growing attention. Among the principal advantages of glass-coated microwires are the most extended diameters range from 100 nm [13] up to 100  $\mu\text{m}$  [23]. Additionally, the presence of flexible, insulating and thin glass-coating together with extended diameters are beneficial for several technical applications [4,24,25].

Similarly to thicker amorphous magnetic wires prepared by in-rotating water technique, magnetic bistability related to remagnetization by fast DW propagation is observed in Fe- and Fe-Ni-rich glass-coated microwires [4,6]. While almost unhysteretic loops with vanishing coercivity and high GMI effect are reported in Co-rich glass-coated microwires [4,6].

As mentioned above, the  $\lambda_s$  of amorphous alloys is principally affected by the chemical composition. Thus, in most commonly studied amorphous  $\text{Co}_{1-x}\text{Fe}_x$  alloys high and positive  $\lambda_s$  (up to  $40 \times 10^{-6}$ ) is reported for Fe-rich compositions, while negative (up to  $-5 \times 10^{-6}$ )  $\lambda_s$  is observed in Co-rich amorphous alloys. Therefore, observed dependence of magnetic properties on chemical composition is commonly attributed to compositional dependence of  $\lambda_s$ .

As discussed above, the  $\lambda_s$  in amorphous materials is affected by stress [8,9]. In the case of glass-coated microwires, the presence of a glass coating associated with the preparation method involving simultaneous solidification of a metallic alloy inside the glass coating leads to an elevated  $\sigma_i$ -value (up to hundreds of MPa) [13–17].

In the case of low-magnetostrictive compositions, where  $\lambda_s(0)$  is approximately of the order of  $10^{-7}$ , and internal stresses are on the order of hundreds of MPa, the second term in Equation (1) becomes comparable to the first term. Consequently, the magnetostriction value and even sign can be substantially different from that of conventional amorphous materials. Therefore, the correct evaluation of  $\lambda_s$ —magnitude in glass-coated microwires becomes a crucial factor for adjusting the magnetic properties of glass-coated microwires and it is relevant for technological applications.

One of the most commonly used methods for evaluation of the  $\lambda_s$  in amorphous materials, is the so called small angle magnetization rotation (SAMR) method [8,9,18]. The magnetostriction of conventional (bulk) magnetic materials usually can be measured by direct methods, such as strain gauge method or the capacitance method [26,27]. However, direct methods require use of the strain gauge or the movable electrode. Therefore, use of such direct methods for  $\lambda_s$  measurements in low dimensional amorphous materials, like amorphous ribbons or wires seems to be difficult. Therefore, indirect methods, like the SAMR method Villari effect or stress dependence of hysteresis loop have been proposed for studied of amorphous low dimensional materials since the 1980s [8,9,18]. Some issues for the use of indirect methods, like the stress dependence of the  $\lambda_s$  in amorphous materials and the influence of mechanical creep deformation of the sample, can be successfully minimized keeping the sample under stress for an as short as possible time [8].

In the case of glass-coated magnetic microwires, the use of direct methods for  $\lambda_s$  evaluation is even more difficult owing to composite origin of glass-coated microwires and substantially lower dimensionality. Therefore, the SAMR method has recently been successfully adapted for magnetic microwires by improved resolution obtained in new experimental set-up [28,29].

Consequently, for glass-coated microwires with elevated internal stresses, studies of the magnetostriction coefficient are essentially relevant both from the point of view of applications and for understanding of the intrinsic properties (the degree of internal stresses relaxation, short range atomic order) of amorphous microwires. Accordingly, this paper presents the experimental results on the magnetostriction coefficient of glass-coated microwires of two different chemical compositions.

## 2. Materials and Methods

We studied  $\text{Fe}_{47}\text{Ni}_{27}\text{Si}_{11}\text{B}_{13}\text{C}_2$  (metallic nucleus diameter,  $d = 29 \mu\text{m}$ , total diameter,  $D = 32.2 \mu\text{m}$ ) and  $\text{Co}_{67}\text{Fe}_{3.9}\text{Ni}_{1.5}\text{B}_{11.5}\text{Si}_{14.5}\text{Mo}_{1.6}$  ( $d = 25.6 \mu\text{m}$ ,  $D = 26.6 \mu\text{m}$ ) glass-coated mi-

crowires produced by Taylor–Ulitsky technique [4,6,15,16,30]. The preparation method of glass-coated microwires consists of melting of the ingot using a high frequency inductor be heating above its melting temperature, and then drawing of a glass capillary filled with the molten metallic alloy. The composite microwire is then wound onto a rotating pick-up bobbin [4,6,30].

The metallic nucleus diameter,  $d$ , has been controlled by the impedance measurements during the preparation [4]. Additionally, an optical microscope Axio Scope A1 was used for the morphology analysis and evaluation of the  $d$  and  $D$ -values of prepared glass-coated microwires. From the images of prepared microwires (see Figure 1a,b), we can clearly see that the metallic nucleus are rather homogeneous and confirm the  $d$  and  $D$ - values.

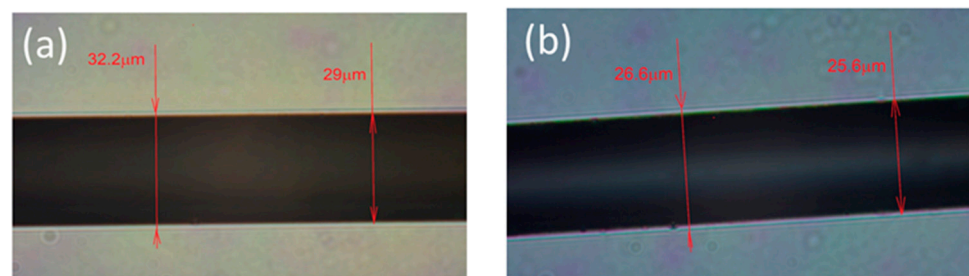


**Figure 1.** Optical microscopy images of  $\text{Fe}_{47}\text{Ni}_{27}\text{Si}_{11}\text{B}_{13}\text{C}_2$  (a) and  $\text{Co}_{67}\text{Fe}_{3.9}\text{Ni}_{1.5}\text{B}_{11.5}\text{Si}_{14.5}\text{Mo}_{1.6}$  (b) samples.

The SAMR method was used to evaluate  $\lambda_s$  in both microwires. This method consists of saturating the sample with an axial magnetic field, while the transverse magnetic field created by AC electric current causes the small angle magnetization rotation [29,30]. When a tensile stress is applied, the magnetization rotation angle decreases due to an increase in the magnetic anisotropy field,  $H_k$ , which leads to a decrease in the amplitude of the second harmonic of the electro-motive force,  $EMF$ , induced in the pick-up coil. Tensile stress,  $\sigma$ , is created by a weight attached to one end of the microwire. The magnetostriction coefficient,  $\lambda_s$ , is then estimated from the  $H_k(\sigma)$  dependence as:

$$\lambda_s = \frac{\mu_0 M_s}{3} \frac{dH_k}{d\sigma_k} \quad (2)$$

where  $\mu_0 M_s$  is the saturation magnetization.

The SAMR method was also used for the evaluation of the  $\lambda_s(\sigma)$  dependence. The detailed description of the set-up developed for the  $\lambda_s$  evaluation in magnetic microwires is provided elsewhere [30].

Hysteresis loops were measured using the fluxmetric method, previously successfully employed for high resolution measurements of axial hysteresis loops of magnetically soft microwires [31]. The 5 cm long samples were placed inside a single layered pick-up coil located inside a 15 cm long solenoid producing an axial homogeneous magnetic field. For this geometry, the influence of the demagnetizing field and hence shape magnetic anisotropy contribution of microwires are negligible. The hysteresis loops have been represented as the normalized magnetization,  $M/M_0$ , versus magnetic field,  $H$ , being  $M$ , the magnetic moment at a given  $H$ , and  $M_0$ , the magnetic moment at the maximum magnetic field amplitude,  $H_0$ . Such  $M/M_0(H)$  loops are useful for comparison of the soft magnetic properties of microwires with different chemical compositions and, therefore, with different saturation magnetization values.

Amorphous structure of as-prepared and annealed samples have been proved by X-ray Diffraction (XRD) using a BRUKER (D8 Advance) X-ray diffractometer with  $\text{Cu K}\alpha$  ( $\alpha = 1.54 \text{ \AA}$ ) radiation. XRD pattern of all the samples (as-prepared and annealed at  $400 \text{ }^\circ\text{C}$ ) present wide halo typical for amorphous alloys (see Figure 2).

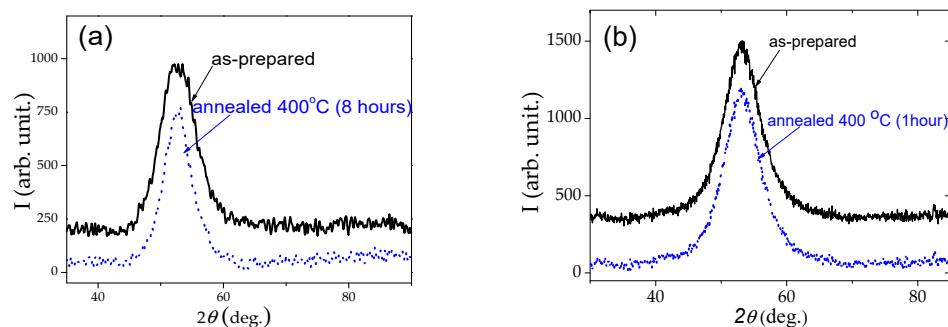


**Figure 2.** XRD patterns of as-prepared and annealed at 400 °C  $\text{Fe}_{47}\text{Ni}_{27}\text{Si}_{11}\text{B}_{13}\text{C}_2$  (a) and  $\text{Co}_{67}\text{Fe}_{3.9}\text{Ni}_{1.5}\text{B}_{11.5}\text{Si}_{14.5}\text{Mo}_{1.6}$  samples (b).

The crystallization and the Curie temperatures,  $T_c$ , of both microwires have been evaluated using the Differential Scanning Calorimetry (DSC) method [32]. We used a DSC 204 F1 Netzsch calorimeter at a heating rate of 10 K/min (in Ar atmosphere).

The determination of the Curie temperature by the DSC method has been reported for more than 20 years [32]. In particular, comparison of the  $T_c$ -values obtained by the DSC with the  $T_c$  obtained by the other commonly accepted methods for  $T_c$  determination, such as temperature dependences of magnetization and electrical resistance, has proved that the turn on DSC curve actually corresponds to the Curie temperature  $T_c$ . An example of the change in the DSC signal in the vicinity of  $T_c$  is provided in Figure 3.

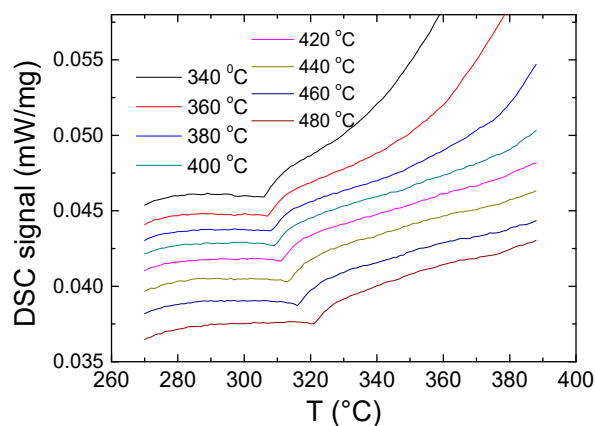


**Figure 3.** Examples of DSC curves in the vicinity of  $T_c$  and their variation with annealing measured for  $\text{Fe}_{73.8}\text{Cu}_1\text{Nb}_{3.1}\text{Si}_{13}\text{B}_{9.1}$  microwire.

In the provided example, it is shown that annealing of microwires leads to a change in the position and the shape of DSC peak in the vicinity of  $T_c$ : with increasing of the annealing temperature it shifts to higher temperatures. Compared to the crystallization peak, the turn in the DSC curve in the vicinity of  $T_c$  looks smaller. However, the use of standard software and a big amount of glass-coated tiny microwires makes it possible to increase the scale of DSC curves and determine  $T_c$  quite accurately [32,33]. Thus, it was demonstrated that the accuracy of  $T_c$  determined from DSC curves is about  $\pm 0.5$  K, which makes this method among the most precise for  $T_c$  determination [32].

### 3. Experimental Results and Discussion

As can be observed from Figure 4, studied microwires present rather different hysteresis loops. A linear and almost unhysteretic loop is observed for  $\text{Co}_{67}\text{Fe}_{3.9}\text{Ni}_{1.5}\text{B}_{11.5}\text{Si}_{14.5}\text{Mo}_{1.6}$  microwire (see Figure 4a), while a rectangular hysteresis loop is observed for  $\text{Fe}_{47}\text{Ni}_{27}\text{Si}_{11}\text{B}_{13}\text{C}_2$  microwire (see Figure 4b). The coercivity,  $H_c$ , of  $\text{Fe}_{47}\text{Ni}_{27}\text{Si}_{11}\text{B}_{13}\text{C}_2$  sample ( $H_c \approx 61$  A/m) is about an order of magnitude higher than that for  $\text{Co}_{67}\text{Fe}_{3.9}\text{Ni}_{1.5}\text{B}_{11.5}\text{Si}_{14.5}\text{Mo}_{1.6}$  microwire ( $H_c \approx 6$  A/m).

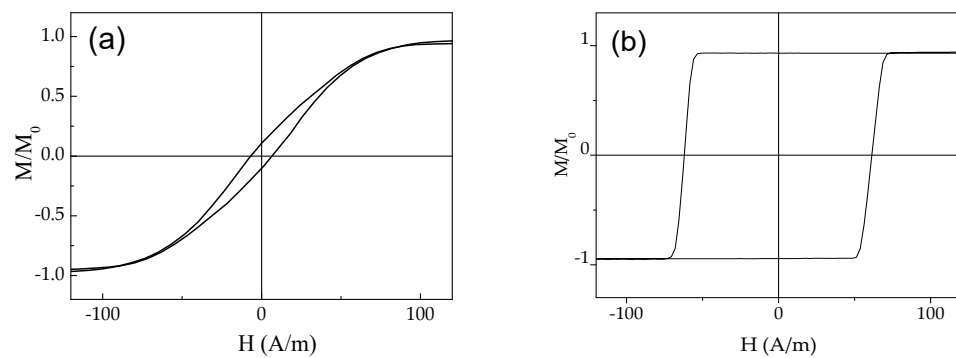


**Figure 4.** Hysteresis loops of  $\text{Co}_{67}\text{Fe}_{3.9}\text{Ni}_{1.5}\text{B}_{11.5}\text{Si}_{14.5}\text{Mo}_{1.6}$  (a) and  $\text{Fe}_{47}\text{Ni}_{27}\text{Si}_{11}\text{B}_{13}\text{C}_2$  (b) samples.

The observed difference in the hysteresis loops of studied microwires can be explained in terms of core–shell domain structure model confirmed experimentally in magnetic microwires with different magnetostriction coefficients [10,21,34–38]. The domain structure of both families (Co-rich and Fe-rich) microwires was extensively studied either by magneto-optical Kerr effect or magneto-optical indicator film methods [34–38]. The core–shell domain structure model describes the domain structure of amorphous magnetic wires as consisting of an inner axially magnetized core surrounded by an outer shell with transverse magnetization. The outer shell of Fe-rich wires has a radial magnetization orientation, while a bamboo domain structure with a circular magnetization orientation is proposed for Co-rich wires [10,21,38]. The difference in the outer shell domain structure is commonly explained considering the interplay of the magnetostriction and internal stresses and different  $\lambda_s$  signs of Fe- and Co-rich magnetic wires. As mentioned above, the axial component of internal stresses arising during the microwires preparation is the largest [14–17]. Consequently, such axial internal stresses produce the transverse magnetic anisotropy in as-prepared Co-rich glass-coated microwires with negative  $\lambda_s$ . In contrast, axial magnetic anisotropy with rectangular hysteresis loops internal stresses appears in Fe-rich microwires with positive  $\lambda_s$ .

From DSC curves, both crystallization,  $T_{cr1}$ , and Curie,  $T_c$ , temperatures can be evaluated (see Figure 5).

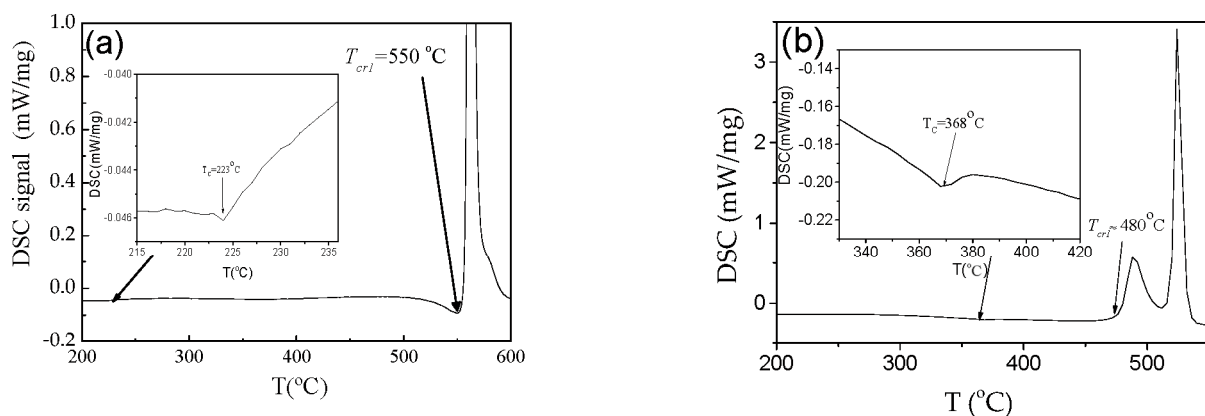


**Figure 5.** DSC curves of  $\text{Co}_{67}\text{Fe}_{3.9}\text{Ni}_{1.5}\text{B}_{11.5}\text{Si}_{14.5}\text{Mo}_{1.6}$  (a) and  $\text{Fe}_{47}\text{Ni}_{27}\text{Si}_{11}\text{B}_{13}\text{C}_2$  (b) samples.

Accordingly, increase in  $H_c$ -value of  $\text{Fe}_{47}\text{Ni}_{27}\text{Si}_{11}\text{B}_{13}\text{C}_2$  sample must be related to different magnetoelastic anisotropy or fine structural rearrangements associated with annealing.

As mentioned in the introduction, in amorphous materials with vanishing  $\lambda_s$ ,  $\lambda_s(\sigma)$  dependence can be relevant [8]. Additionally, one of the main peculiarities of glass-coated microwires is the elevated magnetoelastic anisotropy,  $K_{me}$ , related to the presence of glass-coating [4,7]. As discussed elsewhere [4,7],  $K_{me}$  depends on the magnetostriction coefficient,

$\lambda_s$ , as well as on the total stresses,  $\sigma = \sigma_{\text{appl}} + \sigma_i$ , (being  $\sigma_{\text{appl}}$  and  $\sigma_i$  the applied and internal stresses, respectively) as [4,7]:

$$K_{me} \approx \frac{3}{2} \lambda_s \sigma \quad (3)$$

It is commonly assumed that  $\lambda_s$ -value and sign of amorphous materials are determined by the chemical composition of the alloys. Therefore, for the fixed composition of amorphous microwire, it is expected that the annealing must be the common way allowing diminishing of  $K_{me}$  and hence magnetic softening. However, even for the  $\text{Fe}_{47}\text{Ni}_{27}\text{Si}_{11}\text{B}_{13}\text{C}_2$  microwire, the opposite tendency is generally observed (see Figure 6): some coercivity,  $H_c$ , increasing is observed upon annealing at  $T_{\text{ann}} = 410$  °C. Selected  $T_{\text{ann}}$  is above the Curie temperature,  $T_c$  ( $T_c \approx 360$  °C), and below the crystallization temperature,  $T_{cr}$  ( $T_{cr} \approx 480$  °C).

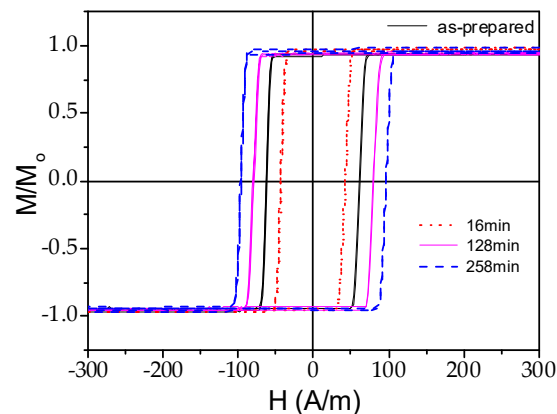


**Figure 6.** Hysteresis loops measured in as-prepared  $\text{Fe}_{47}\text{Ni}_{27}\text{Si}_{11}\text{B}_{13}\text{C}_2$  microwires and annealed at 410 °C for different annealing times.

Similarly, substantial magnetic hardening is observed in  $\text{Co}_{67}\text{Fe}_{3.9}\text{Ni}_{1.5}\text{B}_{11.5}\text{Si}_{14.5}\text{Mo}_{1.6}$  microwire after annealing (see Figure 7). Similarly to  $\text{Fe}_{47}\text{Ni}_{27}\text{Si}_{11}\text{B}_{13}\text{C}_2$  microwire, we used  $T_{\text{ann}} > T_c$  ( $T_c \approx 223$  °C) and  $T_{\text{ann}} < T_{cr}$  ( $T_{cr} \approx 550$  °C). The origin of magnetic hardening of amorphous materials upon annealing has been commonly discussed in terms of the directional ordering of atomic pairs or compositional and topological short-range ordering [39–43]. Correspondingly, directional atomic pair ordering mechanism cannot explain observed magnetic hardening upon annealing of studied microwires.

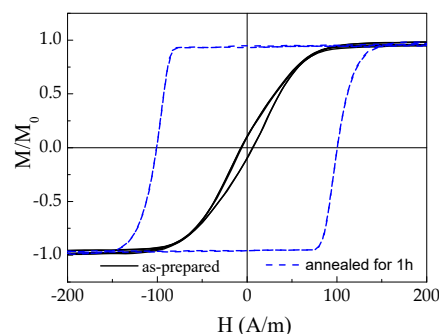


**Figure 7.** Change in the hysteresis loops of  $\text{Co}_{67}\text{Fe}_{3.9}\text{Ni}_{1.5}\text{B}_{11.5}\text{Si}_{14.5}\text{Mo}_{1.6}$  sample after annealing at 400 °C: hysteresis loops of as-prepared (black) and annealed (blue) samples.

For a better understanding of observed magnetic hardening of studied microwires upon annealing, we analyzed the behavior of  $\lambda_s$ -value upon annealing. As can be appreciated from Figure 8, an increase in  $\lambda_s$  is observed in  $\text{Fe}_{47}\text{Ni}_{27}\text{Si}_{11}\text{B}_{13}\text{C}_2$  microwire with annealing time,  $t_{\text{ann}}$ , at  $T_{\text{ann}} > T_c$  ( $T_{\text{ann}} = 400$  and 410 °C). Accordingly, some magnetic hardening of  $\text{Fe}_{47}\text{Ni}_{27}\text{Si}_{11}\text{B}_{13}\text{C}_2$  microwire can be attributed to observed increase in  $\lambda_s$  upon annealing.

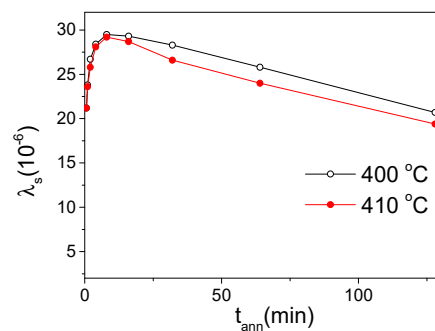


**Figure 8.** Effect of annealing conditions on magnetostriction,  $\lambda_s$ , of  $\text{Fe}_{47}\text{Ni}_{27}\text{Si}_{11}\text{B}_{13}\text{C}_2$  microwire.

A similar tendency, namely an increase in  $\lambda_s$  upon annealing is observed in  $\text{Co}_{67}\text{Fe}_{3.9}\text{Ni}_{1.5}\text{B}_{11.5}\text{Si}_{14.5}\text{Mo}_{1.6}$  microwire (see Figure 9): an increase in  $\lambda_s$ -value is observed for all used  $T_{ann}$ . The most remarkable feature is that it changes not only the  $\lambda_s$ -value but also the sign upon annealing: after a few minutes of annealing,  $\lambda_s$  becomes positive. Such modification of  $\lambda_s$  after annealing can explain the substantial change in the hysteresis loops of  $\text{Co}_{67}\text{Fe}_{3.9}\text{Ni}_{1.5}\text{B}_{11.5}\text{Si}_{14.5}\text{Mo}_{1.6}$  microwire after annealing and magnetic hardening (see Figure 7). As previously shown experimentally, magnetic hardening of Co-rich microwires after annealing is related to the change in domain structure consisting of an increase in the volume of the inner axially magnetized core [4,35].

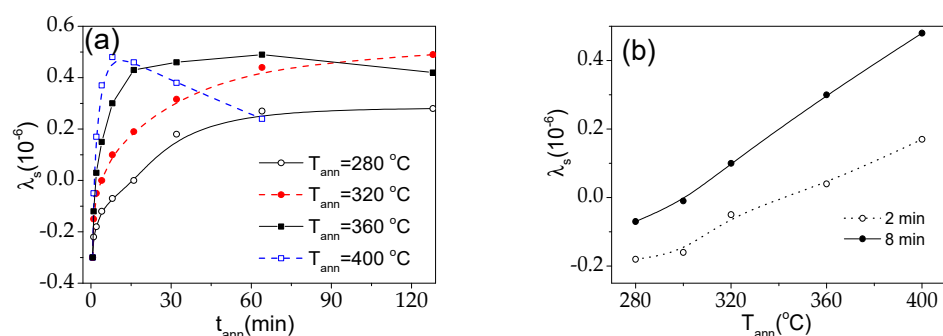


**Figure 9.** Effect of annealing conditions on magnetostriction,  $\lambda_s$ , in  $\text{Co}_{67}\text{Fe}_{3.9}\text{Ni}_{1.5}\text{B}_{11.5}\text{Si}_{14.5}\text{Mo}_{1.6}$  microwire:  $\lambda_s(t_{ann})$  dependencies at different  $T_{ann}$  (a) and  $\lambda_s(T_{ann})$  dependencies at  $t_{ann} = 2$  and 8 min (b).

Additionally,  $\lambda_s$  is affected by both,  $T_{ann}$  and  $t_{ann}$  (see Figure 9a,b). Temperature–time dependencies of various structural and magnetic parameters were previously discussed in terms of structural relaxation involving changes in the atomic short-range order [39–43]. As shown in Figure 9b, an increase in  $\lambda_s$  is affected by both  $T_{ann}$  and  $t_{ann}$ . For  $T_{ann} < 360$  °C only an increase in  $\lambda_s$  is observed for the whole  $t_{ann}$  measured. However, for  $T_{ann} \geq 360$  °C an increase in  $\lambda_s$  is followed by a decrease in  $\lambda_s$  (see Figure 9a). A similar influence of  $T_{ann}$  and  $t_{ann}$  on  $\lambda_s$  was previously reported for Co-Fe rich amorphous ribbons [44], and quite recently in glass-coated microwires (but annealed at only one  $T_{ann}$ ) [45]. The appearance of the maximum on  $\lambda_s(t_{ann})$  dependencies at elevated  $T_{ann}$  was explained by the contribution of two different processes [44].

In the present case of glass-coated microwires, one of such processes must be associated with the internal stresses relaxation upon annealing. The other process must be related with aforementioned changes in in the atomic short-range order.

The Curie temperature,  $T_c$ , is one of the most sensitive magnetic parameters to local structural rearrangements [46–50]. As shown in Figure 10, a substantial and monotonous increase in  $T_c$  is observed for both studied microwires after annealing. Similar dependencies of  $T_c$  upon annealing have been observed in various Fe-, Co- and Ni-rich amorphous alloys [46–48]. Such an increase in  $T_c$  of amorphous alloys upon annealing has been commonly attributed to structural relaxation of amorphous alloys [46–48]. Since, the

magnetostriction of amorphous alloys is linked to the local atomic order, such structural relaxation can be one of the origins of observed  $\lambda_s$  evolution upon annealing.

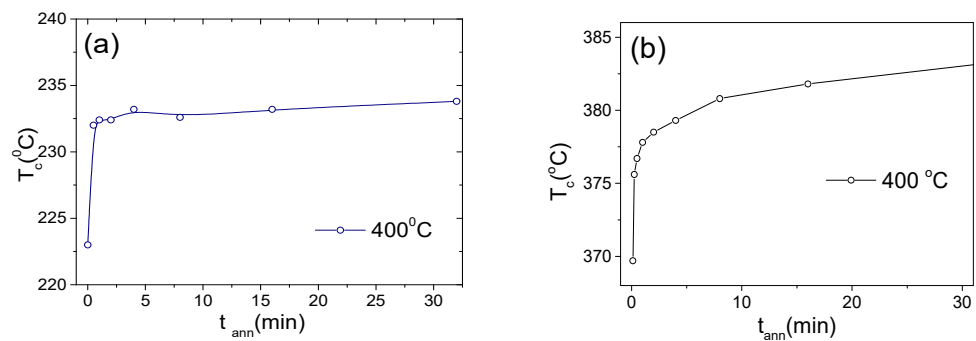


**Figure 10.** Effect of annealing conditions on  $T_c$  of  $\text{Co}_{67}\text{Fe}_{3.9}\text{Ni}_{1.5}\text{B}_{11.5}\text{Si}_{14.5}\text{Mo}_{1.6}$  (a) and  $\text{Fe}_{47}\text{Ni}_{27}\text{Si}_{11}\text{B}_{13}\text{C}_2$  (b) microwires.

From the substantial  $T_c(t_{ann})$  dependence, observed for both studied microwires in Figure 10, we can deduce that structural relaxation processes upon annealing occur in both studied microwires. The detailed description of various atomic mechanisms responsible for the changes in  $T_c$  and other physical properties are provided elsewhere [41,42,49]. Such mechanisms include diffusion of structural defects, topological and compositional short range atomic ordering and clustering [42,43,49,50]. However, the determination of the local atomic structure in amorphous materials by direct methods is a long-standing problem in materials science. Most of the methods allow only average structural information. There are only very few direct observations of local atomic configurations of amorphous materials interpreted as the presence of clusters [51,52].

As mentioned above, one of the commonly involved mechanisms explaining magnetic hardening and magnetic field annealing induced anisotropy of amorphous materials with two or more ferromagnetic elements is atomic pairs ordering consisting of preferential reorientation of atomic pairs under the influence of the local magnetization [39–43,50]. Certainly, a pair of atomic ordering mechanisms can be relevant for both studied microwires with the chemical composition consisting of more than two ferromagnetic elements. However, it is commonly assumed that such mechanism can be relevant for  $T_{ann} < T_c$ . In the case of studied samples, magnetic hardening is observed even upon annealing at  $T_{ann} > T_c$  (see Figures 6 and 7). The dependence of  $T_c$  on  $T_{ann}$  measured in the  $\text{Fe}_{47}\text{Ni}_{27}\text{Si}_{11}\text{B}_{13}\text{C}_2$  microwire reflects the structural relaxation processes upon annealing at  $T_{ann} > T_c$  and  $T_{ann} < T_{cr}$  is provided in Figure 11. Accordingly, various mechanisms previously discussed for amorphous alloys must be involved in observed dependencies of  $T_c$  and  $\lambda_s$  on annealing conditions.

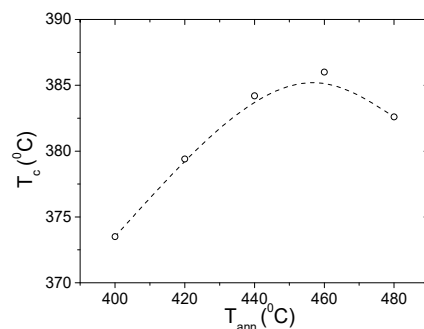


**Figure 11.** Effect of annealing temperature on  $T_c$  of  $\text{Fe}_{47}\text{Ni}_{27}\text{Si}_{11}\text{B}_{13}\text{C}_2$  microwires.

On the other hand, structural relaxation should also be affected by the presence of mechanical stresses: transport processes including diffusion are affected by mechanical stresses [53]. Thus, it was previously reported that the devitrification process (in particular

the  $T_{cr}$ ) and the structure of the crystalline phases are affected by the internal stresses produced by the glass coating [54,55].

One of the peculiarities of glass-coated microwires is the composite structure and a higher level of internal stresses, as compared to the other amorphous materials associated with the presence of a glass coating [6,13–17]. It is worth noting that the internal stresses originated by the difference in the thermal expansion coefficients of metallic nucleus and the glass coating are the largest ones being an order of magnitude higher than the internal stresses related to the rapid melt quenching (typically present in conventional amorphous materials) [14–17]. Additionally, the internal stresses originated by the difference in the thermal expansion coefficients are mostly of tensile (axial) origin [14–17]. Therefore, the  $\lambda_s$ -value and stress-dependence can be rather different from conventional amorphous materials. Thus, one of the reasons for the  $\lambda_s$  modification upon annealing can be related to the internal stresses relaxation. Accordingly, we evaluated the stress dependence of  $\lambda_s$  in both studied microwires.

Similarly to Co-rich amorphous ribbons, a decrease in  $\lambda_s$ , well described as a linear  $\lambda_s(\sigma)$  dependence, is observed in  $\text{Co}_{67}\text{Fe}_{3.9}\text{Ni}_{1.5}\text{B}_{11.5}\text{Si}_{14.5}\text{Mo}_{1.6}$  microwire (see Figure 12a). Phenomenologically, observed  $\lambda_s(\sigma)$  dependence can be described by Equation (1) with a slope,  $B \approx 1.25 \times 10^{-7}$  GPa, quite similar to the B-value, that was previously reported for Co-rich amorphous ribbons [9].

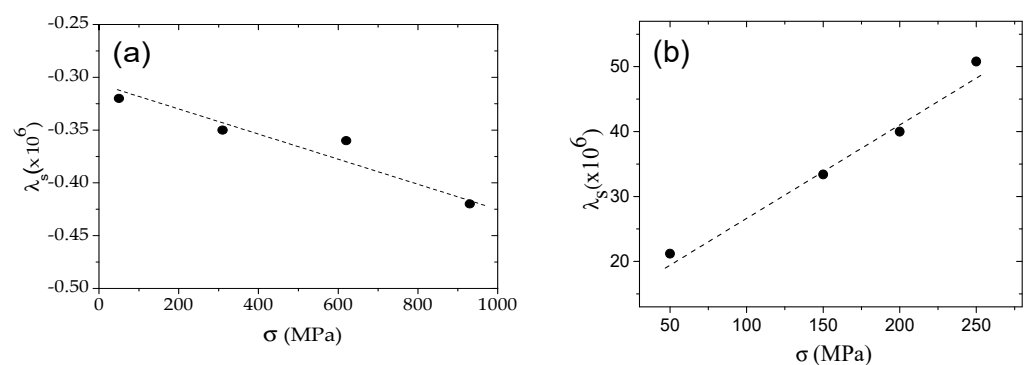


**Figure 12.**  $\lambda_s(\sigma)$  dependence measured in  $\text{Co}_{67}\text{Fe}_{3.9}\text{Ni}_{1.5}\text{B}_{11.5}\text{Si}_{14.5}\text{Mo}_{1.6}$  sample (a) and in  $\text{Fe}_{47}\text{Ni}_{27}\text{Si}_{11}\text{B}_{13}\text{C}_2$  sample (b).

A linear  $\lambda_s(\sigma)$  dependence, is also observed in  $\text{Fe}_{47}\text{Ni}_{27}\text{Si}_{11}\text{B}_{13}\text{C}_2$  microwire; however an increase in  $\lambda_s$  is observed (see Figure 12b). The value of B- coefficient,  $B \approx -1.2 \times 10^{-5}$  GPa, is obtained for  $\text{Fe}_{47}\text{Ni}_{27}\text{Si}_{11}\text{B}_{13}\text{C}_2$  microwire. Previously, negative but rather lower B-coefficient values were observed for annealed Co-rich amorphous materials with positive  $\lambda_s$ -values [9]. However, an increase in  $\lambda_s$  upon application of tensile stress was also recently reported in Fe-Ni-rich microwires with positive  $\lambda_s$  [45].

From the observed  $\lambda_s(\sigma)$  dependencies, we can assume that the internal stresses relaxation can explain only an increase in  $\lambda_s$  for  $\text{Co}_{67}\text{Fe}_{3.9}\text{Ni}_{1.5}\text{B}_{11.5}\text{Si}_{14.5}\text{Mo}_{1.6}$  microwire and a decrease in  $\lambda_s$  for  $\text{Fe}_{47}\text{Ni}_{27}\text{Si}_{11}\text{B}_{13}\text{C}_2$  sample. Therefore, the processes involved in dependence of  $\lambda_s$  on thermal treatment conditions ( $T_{ann}$  or  $t_{ann}$ ) and on applied stress cannot be explained considering only the elevated magnitude of internal stresses for studied microwires.

As mentioned above, the role of local atomic environments is essential for understanding of the magnetostriction coefficient and Curie temperature behavior in glass-coated microwires. Therefore, both internal stresses relaxation and structural (topological or compositional) relaxation upon annealing must be taken into account for interpretation of evolution of magnetostriction upon annealing and applied stresses. One more possible origin of  $\lambda_s(\sigma)$  dependencies in amorphous materials is the so-called “morphic” effect, related to the variation in a saturation elastic constants with the magnetization direction [56,57]. However, the existence of such “morphic” effect is predicted for amorphous materials with near-zero  $\lambda_s$ -values [56].

Most stress sensor applications ideally require materials that demonstrate significant reversible changes in magnetization when subjected to applied stress, while also exhibiting minimal magnetomechanical hysteresis. The dependence of magnetostriction on mechanical stress and annealing temperature can serve as a key starting point for determining the necessary treatment to use an adequate sensitive magneto-transport property, which is crucial for optimizing its sensitivity as a magnetostrictive stress sensor.

#### 4. Conclusions

We evaluated the magnetostriction coefficients and Curie temperature and studied the influence of thermal treatment and applied stresses on magnetostriction coefficient values and the effect of annealing on Curie temperature. Annealing affects the magnetostriction coefficients and Curie temperature of both  $\text{Fe}_{47}\text{Ni}_{27}\text{Si}_{11}\text{B}_{13}\text{C}_2$  and  $\text{Co}_{67}\text{Fe}_{3.9}\text{Ni}_{1.5}\text{B}_{11.5}\text{Si}_{14.5}\text{Mo}_{1.6}$  glass-coated microwires in a similar way. Observed influence of thermal treatment on magnetostriction coefficients and Curie temperature is discussed in terms of internal stresses relaxation and structural relaxation. We observed linear stress dependence of the magnetostriction coefficients in  $\text{Fe}_{47}\text{Ni}_{27}\text{Si}_{11}\text{B}_{13}\text{C}_2$  and  $\text{Co}_{67}\text{Fe}_{3.9}\text{Ni}_{1.5}\text{B}_{11.5}\text{Si}_{14.5}\text{Mo}_{1.6}$  glass-coated microwires with different types of hysteresis loops and positive and low negative magnetostriction, respectively. A decrease with applied stress is observed in  $\text{Co}_{67}\text{Fe}_{3.9}\text{Ni}_{1.5}\text{B}_{11.5}\text{Si}_{14.5}\text{Mo}_{1.6}$  microwire, while an increase in the magnetostriction coefficient is observed in  $\text{Fe}_{47}\text{Ni}_{27}\text{Si}_{11}\text{B}_{13}\text{C}_2$  microwire. Observed dependencies are discussed considering both internal stresses relaxation and short-range atomic ordering. In summary, observed evolution of the magnetostriction upon applied stress and annealing confirms the importance of control of the magnetostriction coefficient for optimization of soft magnetic properties and understanding the origins of the influence of post-processing on magnetic softness in glass-coated microwires.

**Author Contributions:** Conceptualization, A.Z. and V.Z.; methodology, A.Z., M.C., P.C.-L., M.I. and V.Z.; validation, S.K., A.Z., M.C., P.C.-L., S.K. and V.Z.; formal analysis, A.Z., S.K. and M.I.; investigation, A.Z., A.G., P.C.-L., A.G.-G., S.K. and J.O.; resources, A.Z. and V.Z.; data curation, J.O., M.C. and M.I.; writing—original draft preparation, A.Z.; writing—review and editing, A.Z. and P.C.-L.; visualization, M.C. and V.Z.; supervision, A.Z.; project administration, V.Z. and A.Z.; funding acquisition, A.Z. and V.Z. All authors have read and agreed to the published version of the manuscript.

**Funding:** This work was supported by EU under “INFINITE” (HORIZON-CL5-2021-D5-01-06) project, by the Spanish MICIN, under PID2022-141373NB-I00 project and by the Government of the Basque Country under PUE\_2021\_1\_0009, Elkartek (MINERVA, MAGAF and ZE-KONP) projects and under the scheme of “Ayuda a Grupos Consolidados” (ref. IT1670-22). J.O. thanks the Ministry of Higher Education, Science and Technology (MESCYT) of the Dominican Republic.

**Institutional Review Board Statement:** Not applicable.

**Informed Consent Statement:** Not applicable.

**Data Availability Statement:** Data available on request due to restrictions related to the developing projects.

**Acknowledgments:** The authors thank for technical and human support provided by SGIker of UPV/EHU (Medidas Magneticas Gipuzkoa) and European funding (ERDF and ESF). We wish to thank the administration of the University of the Basque Country, which not only provides very limited funding, but even expropriates the resources received by the research group from private companies for the research activities of the group. Such interference helps keep us on our toes.

**Conflicts of Interest:** The authors declare no conflict of interest.

#### References

1. Hasegawa, R. (Ed.) *Glassy Metals: Magnetic Chemical and Structural Properties*; CRC Press: Boca Raton, FL, USA, 1983.
2. Xing, Q.; Lograsso, T.A.; Ruffoni, M.P.; Azimonte, C.; Pascarelli, S.; Miller, D.J. Experimental exploration of the origin of magnetostriction in single crystalline iron. *Appl. Phys. Lett.* **2010**, *97*, 072508. [[CrossRef](#)]

3. Herzer, G. Amorphous and nanocrystalline soft magnets. In Proceedings of the NATO Advanced Study Institute on Magnetic Hysteresis in Novel Materials, Mykonos, Greece, 1–12 July 1996; NATO ASI Series (Series E: Applied Sciences). Volume 338, pp. 711–730.
4. Zhukov, A.; Ipatov, M.; Corte-León, P.; Gonzalez-Legarreta, L.; Blanco, J.M.; Zhukova, V. Soft Magnetic Microwires for Sensor Applications. *J. Magn. Magn. Mater.* **2020**, *498*, 166180. [[CrossRef](#)]
5. Herzer, G. Anisotropies in soft magnetic nanocrystalline alloys. *J. Magn. Magn. Mater.* **2005**, *294*, 99–106. [[CrossRef](#)]
6. Zhukov, A.; Corte-Leon, P.; Gonzalez-Legarreta, L.; Ipatov, M.; Blanco, J.M.; Gonzalez, A.; Zhukova, V. Advanced Functional Magnetic Microwires for Technological Applications. *J. Phys. D Appl. Phys.* **2022**, *55*, 253003. [[CrossRef](#)]
7. Du Tremolet de Lacheisserie, E. *Magnetostriction: Theory and Applications of Magnetoelasticity*; CRC Press: Boca Raton, FL, USA, 1994.
8. Siemko, A.; Lachowicz, H.K. On the Origin of Stress-Dependent Saturation Magnetostriction in Metallic Glasses. *J. Magn. Magn. Mater.* **1990**, *89*, 21–25. [[CrossRef](#)]
9. Barandiaran, M.; Hernando, A.; Madurga, V.; Nielsen, O.V.; Vazquez, M.; Vazquez-Lopez, M. Temperature, stress, and structural-relaxation dependence of the magnetostriction in  $(\text{Co}_{0.94}\text{Fe}_{0.06})_{75}\text{Si}_{15}\text{B}_{10}$  glasses. *Phys. Rev. B* **1987**, *35*, 5066. [[CrossRef](#)]
10. Vazquez, M.; Chen, D.-X. The magnetization reversal process in amorphous wires. *IEEE Trans. Magn.* **1995**, *31*, 1229–1238. [[CrossRef](#)]
11. Sabol, R.; Klein, P.; Ryba, T.; Hvizdos, L.; Varga, R.; Rovnak, M.; Sulla, I.; Mudronova, D.; Galik, J.; Polacek, I.; et al. Novel Applications of Bistable Magnetic Microwires. *Acta Phys. Pol. A* **2017**, *131*, 1150–1152. [[CrossRef](#)]
12. Mohri, K.; Uchiyama, T.; Panina, L.V.; Yamamoto, M.; Bushida, K. Recent Advances of Amorphous Wire CMOS IC Magneto-Impedance Sensors: Innovative High-Performance Micromagnetic Sensor Chip. *J. Sens.* **2015**, *2015*, 718069. [[CrossRef](#)]
13. Chiriac, H.; Lupu, N.; Stoian, G.; Ababei, G.; Corodeanu, S.; Óvári, T.-A. Ultrathin Nanocrystalline Magnetic Wires. *Crystals* **2017**, *7*, 48. [[CrossRef](#)]
14. Antonov, A.S.; Borisov, V.T.; Borisov, O.V.; Prokoshin, A.F.; Usov, N.A. Residual quenching stresses in glass-coated amorphous ferromagnetic microwires. *J. Phys. D Appl. Phys.* **2000**, *33*, 1161–1168. [[CrossRef](#)]
15. Chiriac, H.; Óvári, T.A.; Pop, G. Internal stress distribution in glass-covered amorphous magnetic wires. *Phys. Rev. B* **1995**, *52*, 10104–10113. [[CrossRef](#)] [[PubMed](#)]
16. Zhukova, V.; Blanco, J.M.; Ipatov, M.; Zhukov, A. Magnetoelastic contribution in domain wall dynamics of amorphous microwires. *Phys. B* **2012**, *407*, 1450–1454. [[CrossRef](#)]
17. Torcunov, A.V.; Baranov, S.A.; Larin, V.S. The internal stresses dependence of the magnetic properties of cast amorphous microwires covered with glass insulation. *J. Magn. Magn. Mater.* **1999**, *196–197*, 835–836. [[CrossRef](#)]
18. Narita, K.; Yamasaki, J.; Fukunaga, H. Measurement of magnetostriction of a thin amorphous ribbon by means of small-angle magnetization rotation. *IEEE Trans. Magn.* **1980**, *16*, 435–439. [[CrossRef](#)]
19. Zhukov, A.; Cobeño, A.F.; Gonzalez, J.; Blanco, J.M.; Aragonese, P.; Dominguez, L. Magnetoelastic sensor of level of the liquid based on magnetoelastic properties of Co-rich microwires. *Sens. Actuat. A Phys.* **2000**, *81*, 129–133. [[CrossRef](#)]
20. Praslička, D.; Blažek, J.; Šmelko, M.; Hudák, J.; Čverha, A.; Mikita, I.; Varga, R.; Zhukov, A. Possibilities of Measuring Stress and Health Monitoring in Materials Using Contact-Less Sensor Based on Magnetic Microwires. *IEEE Trans. Magn.* **2013**, *49*, 128–131. [[CrossRef](#)]
21. Mohri, K.; Humphrey, F.B.; Kawashima, K.; Kimura, K.; Muzutani, M. Large Barkhausen and Matteucci effects in FeCoSiB, FeCrSiB, and FeNiSiB amorphous wires. *IEEE Trans. Magn.* **1990**, *26*, 1781–1789. [[CrossRef](#)]
22. Hristoforou, E.; Ktena, A. Magnetostriction and magnetostrictive materials for sensing applications. *J. Magn. Magn. Mater.* **2007**, *316*, 372–378. [[CrossRef](#)]
23. Corte-Leon, P.; Zhukova, V.; Ipatov, M.; Blanco, J.M.; González, J.; Churyukanova, M.; Taskaev, S.; Zhukov, A. The effect of annealing on magnetic properties of “Thick” microwires. *J. Alloys Compd.* **2020**, *831*, 150992. [[CrossRef](#)]
24. Zhukova, V.; Corte-Leon, P.; Blanco, J.M.; Ipatov, M.; Gonzalez, J.; Zhukov, A. Electronic Surveillance and Security Applications of Magnetic Microwires. *Chemosensors* **2021**, *9*, 100. [[CrossRef](#)]
25. Kozejova, D.; Fecova, L.; Klein, P.; Sabol, R.; Hudak, R.; Sulla, I.; Mudronova, D.; Galik, J.; Varga, R. Biomedical applications of glass-coated microwires. *J. Magn. Magn. Mater.* **2019**, *470*, 2–5. [[CrossRef](#)]
26. Brooks, H.A. Magnetostriction vs Co content in amorphous alloys of Fe-Co-P-B-Al. *J. Appl. Phys.* **1976**, *47*, 344–345. [[CrossRef](#)]
27. Tsuya, N.; Arai, K.I.; Shiraga, Y.; Yamada, M.; Masumoto, T. Magnetostriction of amorphous  $\text{Fe}_{0.80}\text{P}_{0.13}\text{C}_{0.07}$  ribbon. *Phys. Stat. Sol. A* **1975**, *31*, 557–561. [[CrossRef](#)]
28. Churyukanova, M.; Semenkova, V.; Kaloshkin, S.; Shuvaeva, E.; Gudoshnikov, S.; Zhukova, V.; Shchetinin, I.; Zhukov, A. Magnetostriction investigation of soft magnetic microwires. *Phys. Stat. Sol. A* **2016**, *213*, 363–367. [[CrossRef](#)]
29. Zhukov, A.; Churyukanova, M.; Kaloshkin, S.; Sudarchikova, V.; Gudoshnikov, S.; Ipatov, M.; Talaat, A.; Blanco, J.M.; Zhukova, V. Magnetostriction of Co-Fe-based amorphous soft magnetic microwires. *J. Electr. Mater.* **2016**, *45*, 226–234. [[CrossRef](#)]
30. Baranov, S.A.; Larin, V.S.; Torcunov, A.V. Technology, Preparation and Properties of the Cast Glass-Coated Magnetic Microwires. *Crystals* **2017**, *7*, 136. [[CrossRef](#)]
31. Gonzalez-Legarreta, L.; Corte-Leon, P.; Zhukova, V.; Ipatov, M.; Blanco, J.M.; Gonzalez, J.; Zhukov, A. Optimization of magnetic properties and GMI effect of Thin Co-rich Microwires for GMI Microsensors. *Sensors* **2020**, *20*, 1558. [[CrossRef](#)]

32. Kaloshkin, S.; Churyukanova, M.; Zadorozhnyi, V.; Shchetinin, I.; Roy, R.-K. Curie temperature behaviour at relaxation and nanocrystallization of Finemet alloys. *J. Alloys Compd.* **2011**, *509* (Suppl. S1), S400–S403. [[CrossRef](#)]
33. Zhukova, V.; Kaloshkin, S.; Zhukov, A.; Gonzalez, J. DSC studies of Finemet-type glass-coated microwires. *J. Magn. Magn. Mater.* **2002**, *249*, 108–112. [[CrossRef](#)]
34. Nderu, J.N.; Takajo, M.; Yamasaki, J.; Humphrey, F.B. Effect of stress on the bamboo domains and magnetization process of CoSiB amorphous wire. *IEEE Trans. Magn.* **1998**, *34*, 1312–1314. [[CrossRef](#)]
35. Zhukov, A.; Chizhik, A.; Ipatov, M.; Talaat, A.; Blanco, J.M.; Stupakiewicz, A.; Zhukova, V. Giant magnetoimpedance effect and domain wall dynamics in Co-rich amorphous microwires. *J. Appl. Phys.* **2015**, *117*, 043904. [[CrossRef](#)]
36. Soldatov, I.; Kolesnikova, V.; Rodionova, V.; Schäfer, R. Interpretation of Kerr Microscopic Domain Contrast on Curved Surfaces. *IEEE Magn. Lett.* **2021**, *12*, 7103804. [[CrossRef](#)]
37. Zhukova, V.; Blanco, J.M.; Chizhik, A.; Ipatov, M.; Zhukov, A. AC-current-induced magnetization switching in amorphous microwires. *Front. Phys.* **2018**, *13*, 137501. [[CrossRef](#)]
38. Orlova, N.N.; Gornakov, V.S.; Aronin, A.S. Role of internal stresses in the formation of magnetic structure and magnetic properties of iron-based glass coated microwires. *J. Appl. Phys.* **2017**, *121*, 205108. [[CrossRef](#)]
39. Luborsky, F.E.; Walter, J.L. Magnetic Anneal Anisotropy in Amorphous Alloys. *IEEE Trans. Magn.* **1977**, *13*, 953–956. [[CrossRef](#)]
40. Haimovich, J.; Jagielinski, T.; Egami, T. Magnetic and structural effects of anelastic deformation of an amorphous alloy. *J. Appl. Phys.* **1985**, *57*, 3581–3583. [[CrossRef](#)]
41. Miyazaki, T.; Takahashi, M. Magnetic annealing effect of amorphous  $(\text{Fe}_{1-x}\text{Co}_x)_{77}\text{Si}_{10}\text{B}_{13}$  alloys. *J. Appl. Phys.* **1978**, *17*, 1755–1763. [[CrossRef](#)]
42. Egami, T. Structural relaxation in amorphous  $\text{Fe}_{40}\text{Ni}_{40}\text{P}_{14}\text{B}_6$  studied by energy dispersive X-ray diffraction. *J. Mater. Sci.* **1978**, *13*, 2587–2599. [[CrossRef](#)]
43. Egami, T. Structural relaxation in amorphous alloys—Compositional short range ordering. *Mater. Res. Bull.* **1978**, *13*, 557–562. [[CrossRef](#)]
44. Hernando, A.; Madurga, V.; Núñez de Villavicencio, C.; Vázquez, M. Temperature dependence of the magnetostriction constant of nearly zero magnetostriction amorphous alloys. *Appl. Phys. Lett.* **1984**, *45*, 802–804. [[CrossRef](#)]
45. Zhukova, V.; Churyukanova, M.; Kaloshkin, S.; Corte-Leon, P.; Ipatov, M.; Zhukov, A. Magnetostriction of amorphous Co-based and Fe-Ni-based magnetic microwires: Effect of stresses and annealing. *J. Alloys Compd.* **2023**, *954*, 170122. [[CrossRef](#)]
46. Zhukova, V.; Blanco, J.M.; Ipatov, M.; Churyukanova, M.; Taskaev, S.; Zhukov, A. Tailoring of magnetoimpedance effect and magnetic softness of Fe-rich glass-coated microwires by stress-annealing. *Sci. Rep.* **2018**, *8*, 3202. [[CrossRef](#)] [[PubMed](#)]
47. Chen, H.; Sherwood, R.; Leamy, H.; Gyorgy, E. The effect of structural relaxation on the Curie temperature of Fe based metallic glasses. *IEEE Trans. Magn.* **1976**, *12*, 933–935. [[CrossRef](#)]
48. Dzhumazoda, A.; Panina, L.V.; Nematov, M.G.; Tabarov, F.S.; Morchenko, A.T.; Bazlov, A.I.; Ukhasov, A.; Yudanov, N.A.; Podgornaya, S.V. Controlling the Curie temperature in amorphous glass coated microwires by heat treatment. *J. Alloys Compd.* **2019**, *802*, 36–40. [[CrossRef](#)]
49. Serebryakov, A.V. Amorphization reactions and glass to crystal transformations in metallic materials. *J. Non Cryst. Solids* **1993**, *156–158*, 594–597. [[CrossRef](#)]
50. Becker, J.J. A new mechanism for magnetic annealing in amorphous metals. *IEEE Tran. Magn.* **1978**, *14*, 938–940. [[CrossRef](#)]
51. Hirata, A.; Guan, P.; Fujita, T.; Hirotsu, Y.; Inoue, A.; Yavari, A.R.; Sakurai, T.; Chen, M. Direct observation of local atomic order in a metallic glass. *Nat. Mater.* **2011**, *10*, 28–33. [[CrossRef](#)]
52. Hirotsu, Y.; Hanada, T.; Ohkubo, T.; Makino, A.; Yoshizawa, Y.; Nieh, T.G. Nanoscale phase separation in metallic glasses studied by advanced electron microscopy techniques. *Intermetallics* **2004**, *12*, 1081–1088. [[CrossRef](#)]
53. Onsager, L. Reciprocal Relations in Irreversible Processes. II. *Phys. Rev.* **1931**, *38*, 2265–2279. [[CrossRef](#)]
54. Zhukova, V.; Cobeño, A.F.; Zhukov, A.; Blanco, J.M.; Larin, V.; Gonzalez, J. Coercivity of glass-coated  $\text{Fe}_{73.4-x}\text{Cu}_1\text{Nb}_{3.1}\text{Si}_{13.4+x}\text{B}_{9.1}$  ( $0 \leq x \leq 1.6$ ) microwires. *Nanostruct. Mater.* **1999**, *11*, 1319–1327. [[CrossRef](#)]
55. Aronin, A.S.; Abrosimova, G.E.; Kiselev, A.P.; Zhukova, V.; Varga, R.; Zhukov, A. The effect of mechanical stress on  $\text{Ni}_{63.8}\text{Mn}_{11.1}\text{Ga}_{25.1}$  microwire crystalline structure and properties. *Intermetallics* **2013**, *43*, 60–64. [[CrossRef](#)]
56. Kraus, L. On the Stress Dependence of the Saturation Magnetostriction in Amorphous Alloys. *Phys. Stat. Sol. A* **1988**, *109*, K71–K74. [[CrossRef](#)]
57. Masow, W.P. A Phenomenological Derivation of the First- and Second-Order Magnetostriction and Morphotropic Effects for a Nickel Crystal. *Phys. Rev.* **1951**, *82*, 715–723.

**Disclaimer/Publisher’s Note:** The statements, opinions and data contained in all publications are solely those of the individual author(s) and contributor(s) and not of MDPI and/or the editor(s). MDPI and/or the editor(s) disclaim responsibility for any injury to people or property resulting from any ideas, methods, instructions or products referred to in the content.